

Millennial-Scale Instability of the Antarctic Ice Sheet During the Last Glaciation

Sharon L. Kanfoush,^{1*} David A. Hodell,^{1*} Christopher D. Charles,²
Thomas P. Guilderson,³ P. Graham Mortyn,²
Ulysses S. Ninnemann^{2,†}

Records of ice-rafted detritus (IRD) concentration in deep-sea cores from the southeast Atlantic Ocean reveal millennial-scale pulses of IRD delivery between 20,000 and 74,000 years ago. Prominent IRD layers correlate across the Polar Frontal Zone, suggesting episodes of Antarctic Ice Sheet instability. Carbon isotopes ($\delta^{13}\text{C}$) of benthic foraminifers, a proxy of deepwater circulation, reveal that South Atlantic IRD events coincided with strong increases in North Atlantic Deep Water (NADW) production and inferred warming (interstadials) in the high-latitude North Atlantic. Sea level rise or increased NADW production associated with strong interstadials may have resulted in destabilization of grounded ice shelves and possible surging in the Weddell Sea region of West Antarctica.

Ice-rafting events in North Atlantic sediments provide evidence for millennial-scale instability of the Laurentide Ice Sheet (LIS) during the last glaciation (1–6). The behavior of the Antarctic Ice Sheet (AIS) on these time scales has not been established, however, despite its relevance to issues of natural and anthropogenic climate change. Much of the West Antarctic Ice Sheet (WAIS) is grounded below sea level and is therefore potentially susceptible to perturbations in sea level and climate (7–9). This inherent instability was also a characteristic of the LIS during the last glaciation, which was grounded below sea level in the Hudson Strait region (2). Under full glacial conditions, the WAIS was about two-thirds larger than the present-day WAIS, sea level was ~120 m lower, and grounded ice shelves in marginal seas around Antarctica were more extensive (9, 10). Thus, the Pleistocene history of the AIS may have included millennial-scale episodes of instability similar to those in the LIS history. If so, sediments offshore Antarctica should record such episodes as layers enriched in IRD.

Pleistocene records of IRD from the Southern Ocean are sparse and have been limited to glacial-interglacial time scales, mostly because of chronological uncertainties (11–13).

General improvements to the dating and chronological resolution of deep-sea sediment cores allowed us to document millennial-scale episodes of IRD delivery to the South Atlantic between 20,000 and 74,000 years ago (20 and 74 ka, respectively) (Table 1). We compared IRD fluctuations in cores along a north-south transect across the Polar Frontal Zone (PFZ) from ~41° to 53°S (Fig. 1). The southernmost record (core TTN057-13/1094) at 53°S is located south of the present-day PFZ and ~2° north of the average winter sea ice limit (14). The intermediate site (core TTN057-10) at 47°S is located within the PFZ, and the northernmost core (TTN057-21) at 41°S is north of the present-day PFZ.

All three cores record discrete episodes of IRD deposition throughout the last glaciation that recur on millennial [~6000- to 10,000-year (~6- to 10-ky)] time scales (Fig. 2 and Table 2). The northernmost and southernmost cores at 41° and 53°S, respectively, share a basic similarity in the timing of prominent IRD peaks (Fig. 3). The core at 47°S in the PFZ, however, contains additional IRD fluctuations and displays peaks of different amplitudes relative to those observed in the other cores. The IRD is composed dominantly of ash and quartz and includes minor amounts of fine-grained volcanics, coarse-crystalline rock fragments, and mica. Geochemical analysis of volcanic ash in nearby cores suggests that it was derived principally from the South Sandwich Islands in the Scotia Arc, with minor contributions from nearby Bouvet Island (11). Volcanic eruptions in the South Sandwich Islands produce ash that is carried east by prevailing winds. The size fraction analyzed (150 μm to 2 mm), however, precludes the inclusion of ash transported to the

core sites by wind or by direct fallout from eruptions. The ash settles on ice shelves in the Weddell Sea and on seasonal sea ice, which acts as a conveyor of ash to the South Atlantic sediments during its seasonal advance and retreat. The quartz and other non-ash lithics are derived from the calving of icebergs off Antarctica (15, 16), which mainly originate today from ice shelves such as those found in the Weddell Sea (17).

There are at least two possible processes that might account for the abrupt oscillations in IRD in South Atlantic sediment cores. Labeyrie *et al.* (16) interpreted increases in quartz between 17 and 35 ka as reflecting increased ice discharge from the AIS. Alternatively, changes in sea surface temperature (SST) in the high-latitude South Atlantic might increase the survivability of icebergs. Keany *et al.* (12) suggested that IRD deposition was related to migration of the PFZ and the zone of rapid melting of icebergs relative to a core's position. Peaks in IRD in Southern Ocean sediments may therefore indicate an increased production of icebergs and/or SST changes that affect their survival. The former has implications for AIS dynamics and predicts similar timing of IRD events across the South Atlantic. Conversely, changes in frontal boundary positions should result in diachronous accumulation of IRD with latitude and a "conjugate region" at intermediate latitudes where the IRD signal is confounded (12).

The Polar Front in the study area is presently located at ~49°S and was apparently displaced northward by ~2° to 4° during the Last Glacial Maximum (18). The winter sea ice limit was displaced northward by ~5° to 8° in relation to its modern position at ~55° in the study area (19). Changes in SST associated with PFZ migrations may have influenced the position of melting of debris-laden icebergs and sea ice in the South Atlantic during the last glaciation, as predicted by Keany *et al.* (12). Thus, we think that the IRD record from 47°S (core TTN057-10) is not solely a record of production of icebergs from the AIS. In contrast, there is no indication that the PFZ migrated north of 45°S during the last glaciation (18), yet the presence of quartz in glacial sediments at 41°S (core TTN057-21) indicates that icebergs reached this distant site. Similarly, the site at 53°S (core TTN057-13/1094) has always been well south of the PFZ and, therefore, the fluctuations in quartz are most probably the result of iceberg production rather than temperature-controlled variations in melting-zone position.

To reconstruct the history of AIS instability, we compared IRD records between cores situated outside the past dynamic range of the PFZ (Fig. 3). IRD concentrations in the South Atlantic decrease with increasing distance from Antarctic source areas, such that abundances at 41°S are about two orders of mag-

¹Department of Geological Sciences, University of Florida, Gainesville, FL 32611, USA. ²Scripps Institution of Oceanography, University of California, San Diego, CA 92093, USA. ³Lawrence Livermore National Laboratory, Livermore, CA 94550, USA, and Department of Earth and Planetary Sciences, Harvard University, Cambridge, MA 02138, USA.

*To whom correspondence should be addressed. E-mail: skanfou@ufl.edu (S.L.K.) and dhodell@geology.ufl.edu (D.A.H.)

†Present address: Borehole Research Group, Lamont-Doherty Earth Observatory, Columbia University, Palisades, NY 10964, USA.

REPORTS

nitude less than that at 53°S (Fig. 2). Even so, the pattern of prominent IRD layers in the two sediment records is remarkably similar (Table 2), and we interpret them as manifestations of increased ice discharge from the AIS. Radiocarbon ages are precise enough to establish that South Atlantic (SA) events SA0 and SA1 are synchronous between the two sites. We cannot prove that the other events are strictly correlative between sites, but the timing is close enough to suggest that the major events represent synchronous deposits. With our most conservative age model, peak SA5 shows a substantial temporal offset between 41° and 53°S, but this offset could be the result of chronological uncertainties in the lower portion of the record from core TTN057-13/1094. Between 10 and 60 ka, we identified five (or possibly six) IRD events that have a temporal spacing that ranges between ~6 and 10 ky (Table 2). This millennial-scale spacing is similar to the 7- to 10-ky recurrence of massive ice discharges associated with Heinrich events in the North Atlantic (1-6).

Comparison of the planktic oxygen isotopic ($\delta^{18}\text{O}$) and IRD signals at 53°S reveals that most, but not all, of the major peaks in IRD closely follow low planktic $\delta^{18}\text{O}$ values (Fig. 4A). These low values represent reduced salinity and/or increased temperature of Antarctic surface waters. During the last deglaciation (termination I), South Atlantic IRD peak SA0 (14.2 to 13.5 ka) correlates to the Antarctic Cold Reversal and global meltwater pulse 1a (~14.4 to 13.7 ka) and may point to an influx of icebergs from the AIS as the cause of these events (20, 21). Peaks SA2 and SA4 coincide with large increases in the abundance of the planktic foraminifer *Neogloboquadrina pachyderma*. The co-occurrence of peaks in IRD and foraminifera in the South Atlantic contrasts with mid-latitude North Atlantic results showing low foraminiferal abundances during Heinrich events (1, 22). Foraminifera and IRD in the Irminger Basin of the high-latitude North Atlantic, however, show a similar relation to that observed in the South Atlantic (23). This may result from iceberg-induced upwelling, as has been reported for increased radiolarian productivity in the Southern Ocean (16, 24), or the retreat of sea ice (23, 25).

To determine the phasing of South Atlantic IRD events relative to variations in the strength of North Atlantic Deep Water (NADW) production and climate in the North Atlantic, we compared the IRD and benthic $\delta^{13}\text{C}$ records in piston core TTN057-21 at 41°S (Fig. 4B). This core was taken on the same sediment drift from which core RC11-83 was recovered and has a stable isotope signal that appears nearly identical in structure to that of RC11-83 (26). Charles *et al.* (27) demon-

strated that the benthic $\delta^{13}\text{C}$ record of core RC11-83 is sensitive to changes in NADW input to the Southern Ocean and bears a

striking resemblance to the $\delta^{18}\text{O}$ of Greenland ice core records. The two records are similar because both the temperature over

Table 1. Eleven ^{14}C dates on acid-leached monospecific samples of *N. pachyderma* from eight stratigraphic levels in piston core TTN057-13-PC4 and the MIS 4/3 boundary (43) were used to constrain the glacial chronology for the spliced TTN057-13-PC4/1094 record. Piston core TTN057-13-PC4 was spliced to Ocean Drilling Program (ODP) core 1094C-2H at a depth of 9.7 m (equivalent to 33,420 ^{14}C years before the present) by adjusting depths in core 1094C-2H upward by 3 m. Two ^{14}C samples, at 9.2 and 11.8 m, were replicated and yielded radiocarbon ages within their respective errors. We chose to construct our age model using dates exhibiting stratigraphic and chronologic internal consistency over the intervals where nearby sample ages are indistinguishable at the 2σ level. This choice does not significantly affect the resulting age model. The ^{14}C dates on samples at and below 11.8 m were not used because this level is below the point where the piston core was spliced to ODP core 1094C-2. Conventional ^{14}C ages shown are uncorrected and without the application of a reservoir effect. Calibrated ages were calculated by applying an 800-year reservoir correction and converting to calendar years using either the method of Stuiver *et al.* (44) or data from Bard *et al.* (45). For the latter, ages were determined by both a least squares regression and a second polynomial fit. Center for Accelerator Mass Spectrometry (CAMS) 52007 is from a 160- μg target and did not yield a finite age.

CAMS	Sample	Depth (cm)	Conventional ^{14}C (years)	Error (years)	Calibrated age (years)	Reference
52002	VII 87-92	473	9,370	± 80	9,600	(44)
50102	VI 0-5	536	10,050	± 40	10,310	(44)
52003	VI 12-17	548	9,970	± 90	10,290	(44)
50103	V 60-62	741	13,140	± 50	14,400, 14,550	(45)
52004	V 81-86	763	13,070	± 80	14,320, 14,470	(45)
50104	IV 90-92	919	26,360	± 150	29,130, 29,980	(45)
50106	IV 90-92REPL.	919	26,360	± 150	29,130, 29,980	(45)
52005	IV 141-143	970	33,420	± 250	36,990, 37,830	(45)
50105	II 50-52	1180	53,720	± 3600	—	—
52006	II 50-52REPL.	1180	52,060	± 2200	—	—
52007	I 50-67	1289	>42,560	—	—	—
—	MIS 4/3	1542	—	—	59,000	(43)

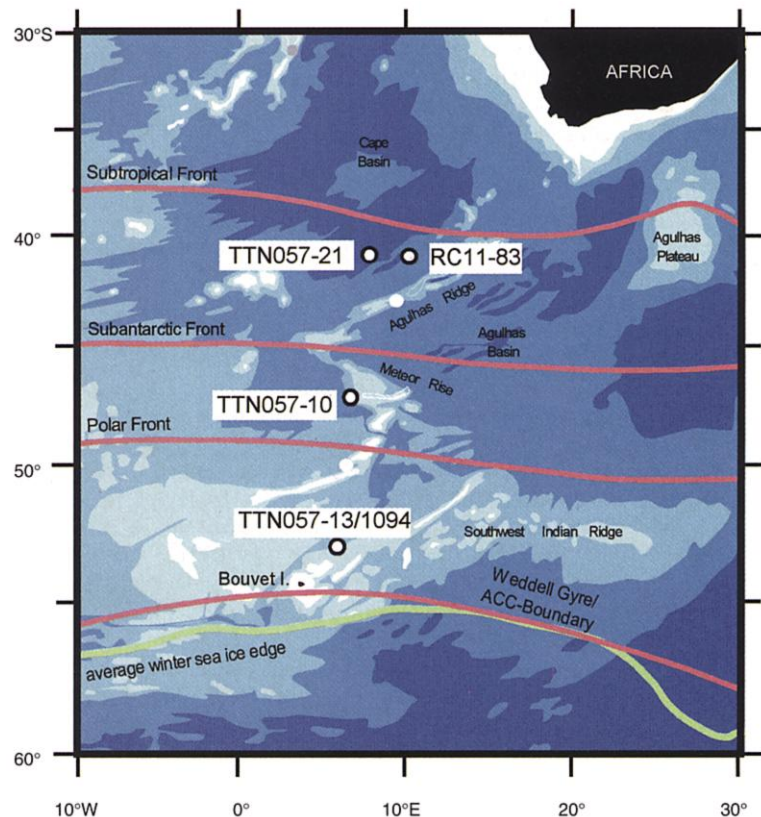


Fig. 1. Site map of the southeast Atlantic indicating the core locations discussed in this study relative to modern positions of important oceanographic boundaries and the winter sea ice margin. Modified after figure F1 in (46).

REPORTS

Greenland and the benthic $\delta^{13}\text{C}$ in the South Atlantic are sensitive to the formation rate of NADW (26, 27). Each of the IRD events

(SA2 through SA5) between 30 and 60 ka is accompanied by an increase in benthic $\delta^{13}\text{C}$, suggesting that South Atlantic IRD events are

associated with strong NADW production and inferred warming in the North Atlantic.

South Atlantic IRD events tend to occur during the strongest interstadials in Greenland (interstadials 8, 12, 14, and possibly 16 and 17) during marine isotopic stage 3 (MIS 3) (28 to 59 ka). Bender *et al.* (28) have suggested that these long interstadial events (>2 ky) in Greenland have counterparts in the Vostok ice core of Antarctica. The South Atlantic events seem to follow a consistent pattern with the exception of peak SA1, which occurred during the Last Glacial Maximum. During the last deglaciation, SA0 occurred synchronously with the Antarctic Cold Reversal (Fig. 4A) and coincides with warming in Greenland associated with the Bolling/Allerod event. The inferred relation between South Atlantic IRD events and warm phases of the Dansgaard-Oeschger (D-O) cycles (29) implies that South Atlantic events were not correlative with North Atlantic IRD deposition because Heinrich events occurred during the coldest phases of the D-O cycles (3–5).

The correlation of South Atlantic benthic $\delta^{13}\text{C}$ maxima and IRD events with interstadials in Greenland argues for an interhemispheric linkage that influenced the stability of the AIS, as opposed to internal ice sheet dynamics (30). Deposition of IRD in the South Atlantic during times of warming in the North Atlantic may be a manifestation of antiphase climate behavior between these regions (31, 32), but not necessarily in the sense normally considered when comparing ice core records of climate. For example, NADW is a major source of heat and salt to the Southern Ocean today (33, 34), and increased production of NADW during warm D-O events may have been responsible for basal melting of expanded Antarctic ice shelves during the last glaciation. Alternatively, sea level rise associated with melting of the LIS during warm D-O phases may have unpinning ice shelves that had grounded on the Antarctic continental shelf during times of lowered sea level (7, 10, 35). Although evidence for the magnitude and timing of sea level variations during MIS 3 is scarce, millennial-scale fluctuations have been proposed on the basis of $\delta^{18}\text{O}$ evidence from the Sulu Sea (36) and uplifted coral terraces on the Huon Peninsula, New Guinea (37). Sea level rise associated with strong interstadial events may not have caused a concurrent unpinning of the LIS because it had already experienced surging and rapid iceberg discharge during the preceding cold D-O phase (i.e., Heinrich Event).

Whereas D-O cycles and Heinrich events appear to have global signatures (38–42), it remains to be seen whether the South Atlantic IRD events identified here will prove to have important regional, hemispheric, or even global implications. As yet, we cannot quantify the volume of ice involved in the rapid calving events or the pattern of discharge in other sec-

Table 2. South Atlantic IRD events and their corresponding calendar ages in cores TTN057-21 (41°S) and TTN057-13/1094 (53°S). Also shown are the age difference and the mean age of events present in both cores. Where observed in both records, the temporal spacing between successive IRD events was calculated with the mean ages.

Event	Age (ka)		Difference (ky)	Mean (ka)	Spacing (ky)
	41°S	53°S			
SA0	14.8	13.6	1.1	14.2	–
SA1	18.3 to 26.5	18.1 to 26.6	1.8	24.5	10.3
SA2	30.9	29.9	1.0	30.4	5.9
SA3	37.1	36.1	1.0	36.6	6.2
SA4	41.7 to 45.1	42.3 to 46.5	1.1	43.8	7.2
SA5	51.2	–	–	–	7.4
SA6	–	55.4	–	–	4.2

Fig. 2. (A) Time series of $\delta^{18}\text{O}$ and weight % of CaCO_3 in cores TTN057-21 (41°S) (green) and TTN057-10 (47°S) (blue) and $\delta^{18}\text{O}$ in core TTN057-13/ODP Site 1094 (53°S) (gold). Oxygen isotopes were measured on planktic foraminifer *Globigerina bulloides* in cores TTN057-21 and RC11-83, whereas *N. pachyderma* (sinistral) was analyzed for $\delta^{18}\text{O}$ in cores TTN057-10 and TTN057-13/1094 in samples where a sufficient number of specimens could be found. The age scale for core TTN057-21 (41°S) was derived by aligning fine-scale features in the isotopic records with those of nearby core RC11-83, which has a well-constrained accelerator mass spectrometry ^{14}C chronology (28, 47). The chronology for core TTN057-10 (47°S) was derived by visual matching of the weight % CaCO_3 record with those of core TTN057-21. The age scale for TTN057-13/ODP Site 1094 (53°S) is given in Table 1. **(B)** Time series of total lithic concentration (blue) and quartz concentration (red) in cores TTN057-21 (41°S), TTN057-10 (47°S), and TTN057-13/ODP Site 1094 (53°S). Lithics were analyzed from the 150- μm to 2-mm size fraction following the methodologies of Allen and Warnke (48). Peaks are dominantly composed of ash and quartz, which were well correlated with each other and with the overall trends in total lithics. Dotted arrows indicate IRD events that correlate across the PFZ. Total lithics and quartz concentrations from 53°S are expressed in 10^3 and 10^2 grains per gram, respectively, in order to enable a comparison of trends in each parameter. Quartz concentration at ~44 ka is off scale at 16×10^2 grains per gram. Ages shown are 10^3 calendar years determined by application of an 800-year reservoir effect and conversion to calendar years using the methods of Stuiver *et al.* (44) and Bard *et al.* (45).

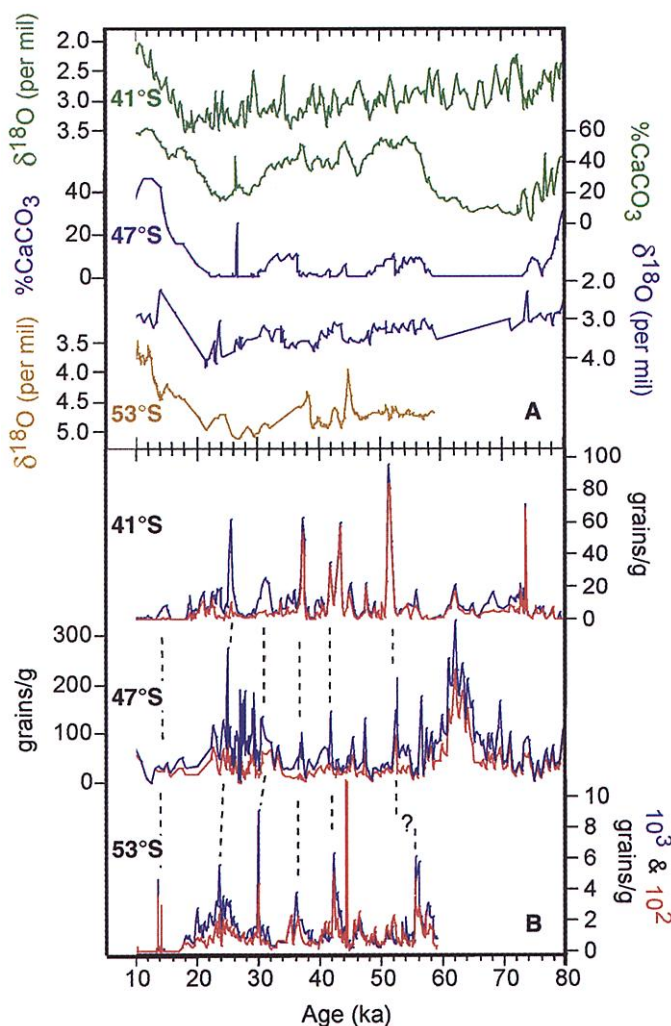


Fig. 2. (B) Time series of total lithic concentration (blue) and quartz concentration (red) in cores TTN057-21 (41°S), TTN057-10 (47°S), and TTN057-13/ODP Site 1094 (53°S). Lithics were analyzed from the 150- μm to 2-mm size fraction following the methodologies of Allen and Warnke (48). Peaks are dominantly composed of ash and quartz, which were well correlated with each other and with the overall trends in total lithics. Dotted arrows indicate IRD events that correlate across the PFZ. Total lithics and quartz concentrations from 53°S are expressed in 10^3 and 10^2 grains per gram, respectively, in order to enable a comparison of trends in each parameter. Quartz concentration at ~44 ka is off scale at 16×10^2 grains per gram. Ages shown are 10^3 calendar years determined by application of an 800-year reservoir effect and conversion to calendar years using the methods of Stuiver *et al.* (44) and Bard *et al.* (45).

Fig. 3. Comparison of total lithic peaks in cores TTN057-21 (41°S) (red) and TTN057-13/ODP Site 1094 (53°S) (blue). Prominent glacial IRD events are assigned the labels of SA1 through SA6. Event SA0 is denoted as such to indicate that it occurs during deglaciation. Brackets illustrate the age range exhibited by IRD peaks within the records from two core sites (41° and 53°S) interpreted here as regionally correlative depositional events. Brackets also denote that some events (especially SA1 and SA4) are composed of several higher frequency peaks.

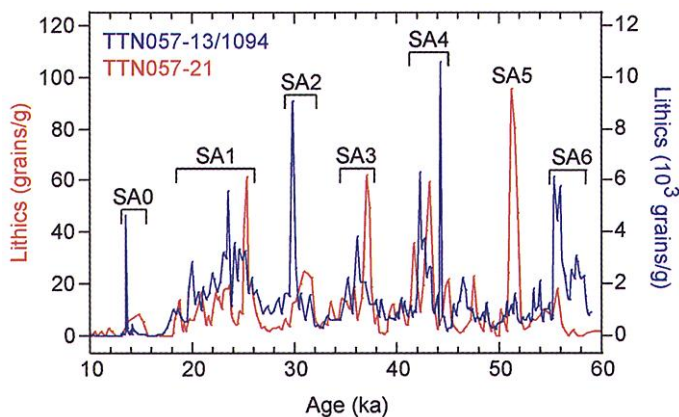
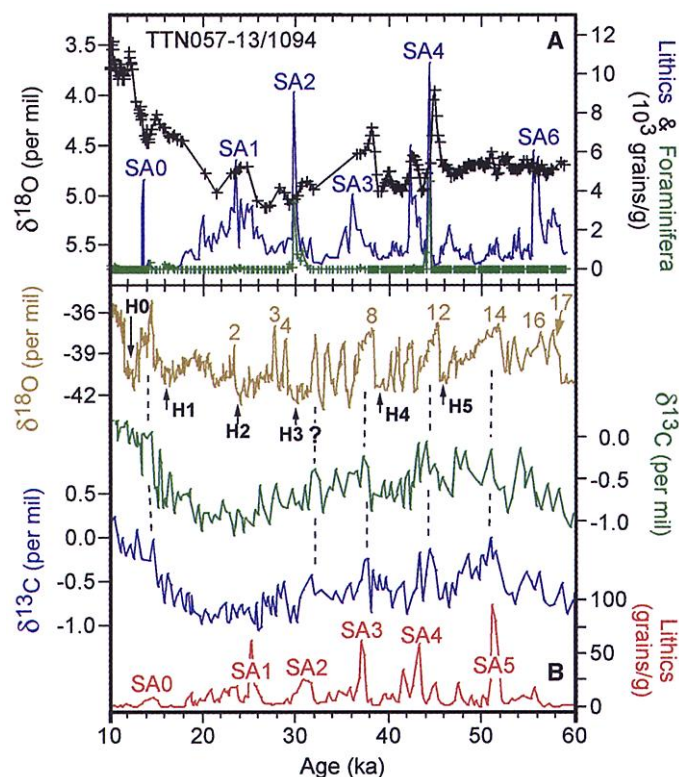


Fig. 4. (A) Total lithic concentration (blue), $\delta^{18}\text{O}$ of *N. pachyderma* (black), and abundance of foraminifera (green) in core TTN057-13/ODP Site 1094 at 53°S. Event SA0 occurs during the Antarctic Cold Reversal, as indicated by an increase in planktic $\delta^{18}\text{O}$ values during Termination I. Events SA1, SA3, and SA4 are associated with low planktic $\delta^{18}\text{O}$ values, which indicate either the influence of meltwater or warm SST. Events SA2 and SA4 are associated with large increases in foraminiferal abundance. (B) Similarities exist between the $\delta^{18}\text{O}$ record of the Greenland Ice Sheet Project 2 (GISP2) ice core (gold) and the benthic $\delta^{13}\text{C}$ (*Cibicidoides*) records of sediment cores RC11-83 (green) and TTN057-21 (blue), with each plotted on their independent chronologies (26, 27). Prominent interstadials as defined in the GISP2 record are numbered, and the North Atlantic Heinrich (H) events are indicated in relation to climatic events in the Greenland ice cores (3, 49). South Atlantic IRD events SA0 through SA5 are expressed as peaks in the total lithic concentration in core TTN057-21 at 41°S (red). Events SA2 through SA5 are each associated with high benthic $\delta^{13}\text{C}$ values, indicating strong NADW production and inferred warming in the North Atlantic.



tors of the Southern Ocean. Nevertheless, the association of IRD events in the South Atlantic during times of increased NADW and warming in the North Atlantic reflect a consistent response to global climate change during the last glaciation.

References and Notes

1. H. Heinrich, *Quat. Res.* **29**, 142 (1988).
2. J. T. Andrews and K. Tedesco, *Geology* **20**, 1087 (1992).
3. G. Bond et al., *Nature* **365**, 143 (1993).
4. G. Bond et al., *Nature* **360**, 245 (1992).

5. G. C. Bond and R. Lotti, *Science* **267**, 1005 (1995).
6. T. Fronval, E. Jansen, J. Bloemendal, S. Johnsen, *Nature* **374**, 443 (1995).
7. G. H. Denton, T. J. Hughes, W. Karlen, *Quat. Res.* **26**, 3 (1986).
8. J. B. Anderson and M. A. Thomas, *Sediment. Geol.* **70**, 87 (1991).
9. R. A. Bindshchadler et al., *Eos Trans. Am. Geophys. Union* **79**, 257 (1998).
10. G. H. Denton and T. J. Hughes, *Quat. Res.* **20**, 125 (1983).
11. J. R. Conolly and M. Ewing, *Science* **150**, 1822 (1965).
12. J. Keany, M. Ledbetter, N. Watkins, T.-C. Huang, *Geol. Soc. Am. Bull.* **87**, 873 (1976).

13. D. W. Cooke and J. D. Hays, in *Antarctic Geoscience*, C. Craddock, Ed. (Univ. of Wisconsin Press, Madison, 1982), pp. 1017–1027.
14. P. Gloersen et al., *Arctic and Antarctic Sea Ice, 1978–1987: Satellite Passive-Microwave Observations and Analysis*, NASA SP-511 (National Aeronautics and Space Administration, Washington, DC, 1993).
15. D. G. Smith, M. T. Ledbetter, P. F. Ciesielski, *Mar. Geol.* **53**, 291 (1983).
16. L. D. Labeyrie et al., *Nature* **322**, 701 (1986).
17. D. A. Warnke, *Am. J. Sci.* **269**, 276 (1970).
18. U. Brathauer and A. Abelmann, *Paleoceanography* **14**, 135 (1999).
19. X. Crosta, J.-J. Pichon, L. H. Burckle, *Paleoceanography* **13**, 284 (1998).
20. J. Jouzel et al., *Clim. Dyn.* **11**, 151 (1995).
21. R. G. Fairbanks, *Nature* **342**, 637 (1989).
22. W. F. Ruddiman, *Geol. Soc. Am. Bull.* **88**, 1813 (1977).
23. M. Elliot et al., *Paleoceanography* **13**, 433 (1998).
24. S. Neshyba, *Nature* **267**, 507 (1977).
25. H. Grobe and A. Mackensen, in *The Antarctic Paleoenvironment: A Perspective on Global Change, Part One*, vol. 56 of *Antarctic Research Series*, J. P. Kennett and D. Warnke, Eds. (American Geophysical Union, Washington, DC, 1992), pp. 349–376.
26. U. S. Ninnemann, C. D. Charles, D. A. Hodell, in *Mechanisms of Global Change at Millennial Time Scales*, vol. 112 of *Geophysical Monograph Series*, P. U. Clark, R. S. Webb, L. D. Keigwin, Eds. (American Geophysical Union, Washington, DC, 1999), pp. 99–112.
27. C. D. Charles, J. Lynch-Stieglitz, U. S. Ninnemann, R. G. Fairbanks, *Earth Planet. Sci. Lett.* **142**, 19 (1996).
28. M. Bender et al., *Nature* **372**, 663 (1994).
29. W. Dansgaard et al., *Nature* **364**, 218 (1993).
30. D. R. MacAyeal, *Paleoceanography* **8**, 775 (1993).
31. W. S. Broecker, *Paleoceanography* **13**, 119 (1998).
32. S. Manabe and R. J. Stouffer, *Paleoceanography* **12**, 321 (1997).
33. S. S. Jacobs, R. G. Fairbanks, Y. Horibe, in *Oceanology of the Antarctic Continental Shelf*, vol. 8 of *Antarctic Research Series*, S. S. Jacobs, Ed. (American Geophysical Union, Washington, DC, 1985), pp. 59–85.
34. A. Gordon, *J. Geophys. Res.* **86**, 4193 (1981).
35. C. L. Hulbe, *Paleoceanography* **12**, 711 (1997).
36. B. K. Linsley, *Nature* **380**, 234 (1996).
37. J. Chappell and N. J. Shackleton, *Nature* **324**, 137 (1986).
38. E. C. Grimm, G. L. Jacobson Jr., W. A. Watts, B. C. S. Hansen, K. A. Maasch, *Science* **261**, 198 (1993).
39. W. S. Broecker, *Nature* **372**, 421 (1994).
40. R. J. Behl and J. P. Kennett, *Nature* **379**, 379 (1996).
41. L. V. Benson et al., *Quat. Res.* **49**, 1 (1998).
42. H. Schultz, U. von Rod, H. Erlenkeuser, *Nature* **393**, 54 (1998).
43. D. G. Martinson et al., *Quat. Res.* **27**, 1 (1987).
44. M. Stuiver et al., *Radiocarbon* **40**, 1041 (1998).
45. E. Bard, M. Arnold, B. Hamelin, N. Tisnerat-Laborde, C. Gabioc, *Radiocarbon* **40**, 1085 (1998).
46. Shipboard Scientific Party, in *Southern Ocean Paleoenvironment*, vol. 177 of *Proceedings of the Ocean Drilling Program, Initial Reports* (Ocean Drilling Program, College Station, TX, 1999), chap. 1, p. 35 (also available at <http://www-odp.tamu.edu/publications/177-IR/177TOC.HTM>).
47. J. E. T. Channell, J. S. Stoner, D. A. Hodell, *Earth Planet. Sci. Lett.* **175**, 145 (2000).
48. C. P. Allen and D. A. Warnke, in *Subantarctic South Atlantic*, vol. 114 of *Proceedings of the Ocean Drilling Program, Scientific Results*, P. F. Ciesielski and Y. Kristofferson, Eds. (Ocean Drilling Program, College Station, TX, 1991), pp. 599–607.
49. P. M. Grootes et al., *Nature* **366**, 552 (1993).
50. The Ocean Drilling Program provided samples for this study with sponsorship from the NSF. This research was supported by U.S. Science Support Program grant F000849 (D.A.H. and S.L.K.), NSF grant OCE-9907036 (D.A.H. and C.D.C.), and a Geological Society of America 1999 grant for graduate student research (S.L.K.). Radiocarbon analyses were performed under the auspices of the U.S. Department of Energy by Lawrence Livermore National Laboratory (contract W-7405-Eng-48). The authors thank anonymous reviewers for suggestions that improved the manuscript.

5 January 2000; accepted 14 April 2000